

Relaxation temperature and storage stability of the functionalized cell wall material residue from lemon peel

5

Novita I. Putri ^{*}, Jelle Van Audenhove, Clare Kyomugasho, Ann Van Loey, Marc Hendrickx ^{**}

Laboratory of Food Technology, Department of Microbial and Molecular Systems, KU Leuven, Kasteelpark Arenberg 22, Box 2457, B-3001, Leuven, Belgium



ARTICLE INFO

Keywords:
 Cell wall material
 Glass transition
 Structural relaxation
 Storage stability

ABSTRACT

Lemon peel cell wall material (CWM) residue obtained after acid pectin extraction can be functionalized into a texturizing ingredient using mechanical treatments such as high-pressure homogenization. The application of CWM as a texturizing ingredient is most likely through a dry powder and thus the stability of its functionality (rheological property) during storage becomes an obvious question. However, studies on the glass transition properties of this CWM residue and its relation to storage stability are largely lacking. This study aims to first evaluate the potential of two methods, i.e. DSC analysis and combined TMCT-DMTA (thermal mechanical compression test – dynamic mechanical thermal analysis) to measure the Tg and relaxation temperature of lemon peel CWM and subsequently relate the results to the stability of the material's rheological property. The results showed that DSC-based Tg measurements may not be the most appropriate indicator for storage stability of the lemon peel CWM residue, despite being the most commonly used method to explain state transition in materials. On the other hand, the structural relaxation phenomena elucidated by the change in mechanical properties measured by TMCT-DMTA correlated with the results of storage stability of the material. To ensure the stability of the CWM residue, storage should be carried out at conditions (temperature and moisture content) before the onset of $\tan \delta$ curve change. In conclusion, relaxation phenomena observed through the measurement of mechanical properties, in particular the $\tan \delta$ curve from DMTA, provides a suitable starting point for inferring the stability of the functionalized CWM residue.

1. Introduction

Lemon peel, by-products from the citrus processing industry, is produced in relatively high amounts which puts a significant burden on the environment. An efficient by-product management strategy is needed to minimize its environmental impact and to increase the overall valorization. To date, the extraction of citrus pectin, an ingredient widely used as thickening agent in food production, is the most widely implemented valorization route of lemon peels. However, the industrial pectin extraction process leaves another significant amount of fiber-rich material. Previous studies have shown that suspensions prepared from the residue left after acid pectin extraction (AR) have excellent rheological properties (high storage modulus), especially after mechanical treatment such as high pressure homogenization (HPH) (Putri et al., 2022; Willemse et al., 2017). The functionalization with HPH caused changes on the microstructure of the AR particles, including

fragmentation (size reduction) and aggregation. The aggregation formed a network which entraps water, creating a gel-like structure in suspension. This means that the functionalized pectin-depleted residue has a high potential as a texturizing ingredient, therefore a study of this ingredient's stability during storage becomes necessary.

The concept of glass transition temperature (Tg) has been used widely to predict the stability of foods and food ingredients (Sablani et al., 2007). When a material is in its glassy state (at a temperature below the Tg), it is regarded as stable due to its limited molecular mobility. Contrary, when a material is put into a condition (temperature-moisture combination) above its Tg, the rate of physical, chemical and biological changes largely increases and the material becomes unstable (Champi et al., 2000). The glass transition phenomena can be perceived from changes in the thermal and mechanical properties of the material as it is heated/cooled. The most common method to determine the Tg of a material is by measuring the change in the heat capacity

* Corresponding author.

** Corresponding author.

5 E-mail addresses: novitaika.putri@kuleuven.be (N.I. Putri), jelle.vanaudenhove@kuleuven.be (J. Van Audenhove), c.kyomugasho@yahoo.com (C. Kyomugasho), ann.vanloey@kuleuven.be (A. Van Loey), marc.hendrickx@kuleuven.be (M. Hendrickx).

using differential scanning calorimetry (DSC). However, the changes in the thermal properties of some food materials, such as the cell wall material (CWM), can be very small during the transition, making it difficult to detect (Boonyai et al., 2006; Roos, 1998). Therefore, in this study, the T_g of the functionalized lemon peel residue after pectin extraction was measured by both the change in thermal and mechanical properties.

To date, only few studies are available on CWM stability during storage and moreover studies on pectin-depleted CWM, to the best of our knowledge, are not existing. The available studies on fiber-rich materials (Fernandez-Lopez et al., 2009; Sharma et al., 2017) mostly demonstrate the degradation of fiber quality during storage without correlating it to the concept of molecular mobility and glass transition, possibly due to the limitation of the T_g analysis. The quality degradation could be attributed to the collapse of the material due to moisture absorption (Fernandez-Lopez et al., 2009). Collapse happens when a material loses its structure and volumetric shrinkage occurs causing loss of porosity (Levi & Karel, 1995). Collapse of amorphous food materials, occurs because of a solid flow resulting from a decreasing viscosity whereby the matrix is no longer capable to support and carry its own mass (Fan & Roos, 2017). This solid flow arises from an increased molecular mobility. However, the characterization of the molecular mobility and its relation to the storage stability of CWM has not been extensively studied. Therefore, this study attempts to fill this gap by describing the molecular mobility of CWM based on the changing mechanical properties and how these changes relate to the functionality (specifically rheological property) of the material.

This study aims to include the different methods to measure T_g and relaxation temperature of lemon peel CWM residue and relate them to the stability of the material's rheological property as influenced by storage. An understanding of how the material behaves during storage may encourage its application in industry and support the effort to valorize the residue of lemon peel after pectin extraction.

2. Materials and methods

2.1. Materials

Dry and milled lemon peel (LP) powder was provided by Cargill R&D Centre Europe (Vilvoorde, Belgium). All the chemicals used for moisture content equilibration were of analytical grade.

2.2. Dried functionalized Acid Residue preparation

The dry LP was treated to obtain the Alcohol Insoluble Residue (AIR) and subsequently pectin was extracted from the AIR using nitric acid at pH 1.6, 80 °C for 1 h. The unextractable fraction was collected as Acid Residue (AR). The AR was then resuspended at 2% solid concentration, the pH was adjusted to 4.5 and then high pressure homogenized at 20 MPa (Panda 2k NS 1001L, GEA Niro Soavi, Parma Italy). All these procedures have been described in detail in our previous studies (Putri et al., 2022; Willemsen et al., 2017). After HPH, the functionalized AR was air-dried after water-alcohol exchange. For this, the functionalized AR was mixed with technical ethanol 99% at a 1:4 (v/v) ratio for 10 min and then allowed to stand for 60 min. This mixture was vacuum filtered (Machery-Nagel MN 615). A second round of alcohol-water exchange was carried out with the technical ethanol 99% at the ratio of 1:1 from initial volume of material. This mixture was allowed to stand for 30 min, and vacuum filtered. The solids after filtration were air-dried overnight to obtain the dried functionalized AR. The moisture content after drying was 11.1 ± 1.1 % w.b. The dried functionalized AR was kept in vacuum bags in a freezer at -40 °C until further use.

2.3. Composition analysis of the samples

The composition of both AIR and functionalized AR was determined

by neutral sugar analysis (using HPAEC-PAD), galacturonic acid content analysis (using spectroscopy) and protein content analysis (using combustion method). The analyses were carried out in triplicates using the method explained in our previous study (Putri et al., 2022).

2.4. Moisture content equilibration and sorption isotherm

In order to achieve various moisture content, the AIR and functionalized AR powder were stored at 4 °C for at least 3 weeks in containers with P_2O_5 (a.w. 0.00) or saturated salt solutions: LiBr (a.w. 0.07), LiCl (a.w. 0.12), CH_3COOK (a.w. 0.24), $MgCl_2$ (a.w. 0.34), K_2CO_3 (a.w. 0.43), $Mg(NO_3)_2$ (a.w. 0.59), NaBr (a.w. 0.64), KI (a.w. 0.73) and KCl (a.w. 0.87) (Greenspan, 1976). The moisture content of the material was measured at the end of the equilibration period by gravimetric analysis. The moisture sorption isotherm was obtained and fitted to the GAB equation (see below) by non-linear regression.

$$W = \frac{CKW_m a_w}{(1 - Ka_w)(1 - Ka_w + \frac{8}{3}Ka_w)} \quad (eq.1)$$

W is the equilibrium moisture content of the material on dry basis and a_w is the water activity. W_m , C and K are the fitted constants. W_m represents the amount of water adsorbed in the monolayer. The W_m value indicates the availability of active water sorption sites on the material. C represents the strength of water binding with a larger C value indicating a stronger binding of water in the monolayer. K is a correction factor, when K approach one, there is no distinction between the water molecules beyond the monolayer and pure water (Quirijns et al., 2005).

2.5. Molecular mobility analysis with different methods

2.5.1. Differential scanning calorimetry

A Differential Scanning Calorimeter Q-2000 (TA instruments, USA) was used to scan the thermal behavior of AIR and functionalized AR powder with different moisture contents. Approximately 20 mg of the powder was weighted into hermetically sealed T_{zero} aluminium pans. An empty pan was used as a reference and two cycles of heating-cooling were carried out, first from -60 °C to 90 °C and second from -60 °C to 120 °C, both at a rate of 6 °C/min. Glass transition temperature, further referred to as T_g , was defined as the mid-point of the transition range observed in the heat flow curve of the second heating cycle (Kymugasho et al., 2021; Pelgrom et al., 2013). An example of such heat flow curve and the analysis of the transition is presented in the Supplementary Materials (Figure S-1). The analysis was carried out in triplicate.

2.5.2. Thermal mechanical compression test - dynamic mechanical thermal analysis

Combined TMCT-DMTA analyses were carried out according to the methods described in Aravindakshan et al. (2022) using an Anton Paar MCR302 rheometer (Graz, Austria) equipped with a CTD450 oven. Approximately 2 g of the sample (AIR or functionalized AR powder) was loaded into the measuring system (cylindrical cup Ø 22 mm; cylindrical bob Ø 20 mm) and the oscillation-compression force was applied at normal force 30 N, shear strain 0.05% and frequency 1 Hz. The temperature scan spanned -60 °C- 120 °C at the rate of 2 °C/min.

From the TMCT-DMTA data, two different values of relaxation temperature were obtained. First, the relaxation temperature from TMCT analysis (Tr-TMCT), determined based on the change of the sample compressibility due to the normal force by measuring the displacement of the probe during the heating scan (with correction of the measuring system's thermal expansion from a scan on microcrystalline cellulose). Secondly, relaxation phenomena from the DMTA were based on the change of the ratio between loss and storage modulus (or loss factor, $\tan \delta$) obtained using oscillatory shear measurements.

2.5.3. Gordon-Taylor equation fitting

The T_g values obtained from DSC and relaxation temperature from TMCT analysis (Tr-TMCT) were fitted into the Gordon-Taylor (G-T) equation below using non-linear regression analysis.

$$T = \frac{T_s \times X_s + X_w \times T_w \times k}{X_s + X_w \times k} \quad (\text{eq. 2})$$

where s denotes the solid fraction (CWM) of the sample, w denotes the water fraction, T is the temperature of transition or relaxation, T_w is the glass transition temperature of water = 6.135 °C, X is the mass fraction and k is the constant that corresponds to the plasticizing effect of water on the material.

2.6. Storage study setup

A storage study was set up for the dried functionalized AR based on the results of the DSC and TMCT-DMTA analysis. Various storage conditions were identified to encompass various states of the functionalized AR, from stable to unstable. A combination of three moisture contents (11%, 14% and 16% w.b.) and three storage temperature (10, 25, and 40 °C) was used. An additional temperature condition (-10 °C) was used to store the material at 16%w.b. moisture content to ensure that storage at an anticipated stable condition was well covered. To adjust the moisture content prior to the storage study, the functionalized AR were equilibrated in airtight containers above saturated salt solutions (MgCl₂, MgNO₃ and KI) for 5 weeks. After moisture equilibration, the functionalized AR were packed into inert glass jars with minimum headspace to prevent moisture exchange and stored for 2, 5 and 14 weeks. At the end of each storage period, the dried functionalized AR samples were regenerated (in duplicate) into 2% w/w solid suspensions. The regeneration was done by letting the material stand in water for 1 h and followed by mixing using L5M-A mixer with an emulsion screen work-head (Silverson, East Longmeadow, MA, USA) at 4300 RPM for 10 min. The rheological properties of these suspensions were measured as an indicator of the material's functionality.

The results of the storage study were fitted by non-linear regression using a first order fractional conversion model:

$$G'(t) = G'_f + (G'_i - G'_f) e^{-kt} \quad (\text{eq. 3})$$

where G'_f is an estimated final extent of functionality loss, G'_i is the average initial value of G' observed, t is the storage time (week) and k is the reaction rate constant.

2.7. Rheological property analysis

The rheology of the CWM suspension was analyzed using the method according to (Willemsen et al., 2018). An Anton Paar MCR302 rheometer (Graz, Austria) equipped with a custom-built cup and concentric cylinder with conical bottom was used. The gap between the cylinder and the cup was 2 mm. Strain sweep (at ω 1 Hz and strain 0.01%–100%) was done to determine the linear viscoelastic region and a frequency sweep (at ω 100 to 0.1 Hz and strain 0.1%) was carried out at 25 °C. Rheology analysis was carried out in duplicate, each with newly loaded samples.

2.8. Statistical analysis

Significant statistical difference ($\alpha = 0.05$) between model-fitting parameter were determined by confidence interval calculation. GAB and G-T curve fitting was carried out in JMP Pro 17 statistical software (SAS Institute Inc, Cary, NC, USA) and fractional conversion model fitting for the storage study results was done in SAS statistical software (SAS Institute Inc, Cary, NC, USA).

3. Results and discussions

3.1. Composition of AIR and functionalized AR

The monosaccharides that comprise the CWM samples (both AIR and functionalized AR) and their protein content are presented in Table 1. Both AIR and functionalized AR are mainly composed of cell wall polysaccharides, i.e. cellulose, hemicellulose and pectin. A small portion of protein (5–7% d.b.) was detected in both AIR and functionalized AIR. The main difference between AIR and functionalized AR is the galacturonic acid content, which can be an indicator of pectin content. Since functionalized AR underwent pectin extraction process in order to increase the CWM functionality as texturizing ingredient (Putri et al., 2022), approx. 50% d.b of the pectin was removed. Consequently, the proportion of cellulose and hemicellulose, as indicated by the glucose, xylose and galactose content, in the functionalized AR sample increased.

3.2. Isotherm sorption of the materials

The relation between water activity and moisture content (moisture sorption isotherm) is an important characteristic in the study of the stability of low-moisture food product (Koç et al., 2010; Lee & Robertson, 2022; Sant'Anna et al., 2014). The moisture sorption isotherm (at 4 °C) for both materials in the present study, AIR and functionalized AR from lemon peel, is shown in Fig. 1. Both materials showed a type II behavior according to the Brunauer-Emmet-Teller classification, which is frequently found in food products (Andrade P. et al., 2011). The experimental data was fitted to the GAB equation and the estimated value for the parameters are shown in Table 2. Both AIR and functionalized AR showed similar C and K values but significantly different monolayer values (W_m). AIR had a significantly higher W_m which indicating that it has more active (or better accessible) water sorption sites. This is also shown in the moisture sorption isotherm graph, in which AIR had higher moisture content at a given a_w value compared to the functionalized AR. This difference is expected since AIR contained more hygroscopic components, such as low molecular weight compounds and pectin, that were partially extracted for the functionalized AR. It has been largely acknowledged that the composition of the materials affected the moisture sorption capacity (Sormoli & Langrish, 2015; Timmermann et al., 2001). The sorption isotherm data at 4 °C were used to prepare samples at specific moisture contents in view of the T_g /Tr measurements and the storage experiment.

3.3. Glass transition and structural relaxation of the cell wall material from lemon peel

3.3.1. Differential scanning calorimetry (DSC)

DSC is one of the commonly used methods to measure T_g . It measures the transition in the thermal properties of the material by measuring the change of specific heat (Le Meste et al., 2002). However, DSC was not sensitive enough to measure the T_g of the functionalized lemon peel AR. On the other hand, transition in the DSC thermogram, albeit weak and broad, was observed for lemon peel AIR, except for samples with very low moisture content (<9% w.b.). AIR contains larger amounts of components that may contribute to the thermal glass transition, for example sugars, oligosaccharides, or acids. These components were extracted from the AIR during the AR preparation and consequently, the functionalized AR from lemon peel contains mainly cellulose and the other biopolymers such as pectin and hemicellulose (Table 1). The change in the heat capacity occurring over the glass transition of biopolymers is relatively small and therefore difficult to be captured by DSC (Roos, 1998; Sablani et al., 2010). Consequently, the DSC results could not provide precise specific transitions for food containing predominantly component with large molecular weight, such as the functionalized AR. Therefore, to describe the glass transition phenomena of CWM residues with DSC, the data from the AIR samples at higher moisture

Table 1Compositions of AIR and functionalized AR (g/100 g dry matter). Values presented are mean \pm standard deviation (n = 6).

Sample	Fucose	Rhamnose	Arabinose	Galactose	Non-cellulosic Glucose	Cellulosic Glucose	Xylose	Mannose	Galacturonic acid	Protein
AIR	0.21 \pm 0.06 ^a	1.45 \pm 0.38 ^a	14.48 \pm 1.82 ^a	6.83 \pm 2.16 ^a	6.87 \pm 0.92 ^a	19.29 \pm 4.31 ^a	4.13 \pm 1.59 ^a	2.67 \pm 0.58 ^a	35.80 \pm 0.44 ^a	5.73 \pm 0.49 ^a
Functionalized AR	1.03 \pm 0.62 ^a	0.80 \pm 0.34 ^b	2.91 \pm 0.50 ^b	11.32 \pm 4.10 ^b	6.12 \pm 2.29 ^a	58.48 \pm 2.21 ^b	12.03 \pm 3.59 ^b	5.94 \pm 1.90 ^b	16.50 \pm 0.51 ^b	7.36 \pm 0.11 ^b

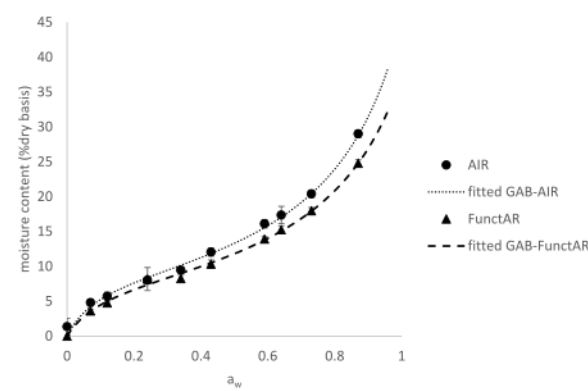


Fig. 1. Moisture Sorption isotherm at 4 °C for AIR and functionalized AR from lemon peel.

Table 2

GAB parameters of moisture sorption isotherm.

Materials	W _m	C	K
AIR	8.76 \pm 0.52 ^a	13.92 \pm 3.53 ^a	0.81 \pm 0.02 ^a
Functionalized AR	8.04 \pm 0.43 ^b	12.26 \pm 2.46 ^a	0.79 \pm 0.02 ^a

content ($\geq 9\%$ w.b.) are used in this study.

The mid-point of the transition shown in the thermogram of the second heating cycle of AIR samples was identified as its Tg-value. The Tg of the AIR sample in function of dry matter content is presented in Fig. 2. Despite the insensitivity of the DSC method for Tg measurement of CWM, few studies reported Tg values for papaya (Nieto-Calvache et al., 2019) and carrot CWM (Georget et al., 1999), with similar and slightly higher Tg compared to lemon peel AIR, respectively. As the moisture content of the lemon peel AIR increased, the Tg decreased, which is a common behavior in many biological materials. It is a well-established fact that water acts as a plasticizer and causes a

depreciation of Tg in low moisture food (Le Meste et al., 2002; Roos, 1998). Previous studies also showed this moisture plasticizing effect in fiber-rich material obtained from apple pomace and carrot (Georet et al., 1999; Zlatanović et al., 2019). The value of Tg in function of dry matter content of the lemon peel CWM were fitted to G-T equation and the parameters obtained, T_s and k, are presented in Table 3. The moisture plasticizing effect (as indicated by the k value of G-T equation) measured by DSC was 4.81, which is similar to other fruit- and vegetable-based food materials and food products (Fongin et al., 2017; Stepień et al., 2020).

3.3.2. Thermal mechanical compression test – dynamic mechanical thermal analysis (TMCT-DMTA)

Contrary to the DSC method, the TMCT-DMTA managed to clearly show structural relaxation phenomena in both lemon peel AIR and functionalized AR. This supported the well-established fact that the mechanical property analysis is more sensitive in measuring the transition or relaxation phenomena in food products (Roos, 1998). TMCT-DMTA analysis reveals structural relaxation phenomena based on the change in the material's mechanical properties, more specifically the compressibility and the moduli obtained from oscillatory shear analysis. As the result of the TMCT-DMTA is highly dependent on the measurement frequency (Le Meste et al., 2002), please note that all the structural relaxation temperatures described here are based on measurement at frequency 1 Hz.

Tr-TMCT in function of dry matter content for both AIR and functionalized AR is shown in Fig. 3. Representative Δ gap curves used for the calculation of Tr-TMCT are presented in the Supplementary Materials (Figure S-2). AIR and functionalized AR have similar values of Tr-TMCT and show similar changes due to the moisture plasticizing effect. The values of Tr-TMCT slightly decreased as the sample's moisture content increased. However, the moisture plasticizing effect on the TMCT (and DMTA) in this study was very limited, especially if compared to the plasticizing effect on the thermal transition. The mechanism of the moisture plasticizing effect on the structural relaxation of glassy biopolymers, especially amorphous carbohydrates (using maltodextrin as an example), has been proposed (Kurn et al., 2004). First, the absorbed water would fill small voids in the glassy matrix of the material, changing the matrix free volume. Second, the water would interfere with intermolecular hydrogen bonds, increasing the degree of freedom of the carbohydrate molecules and eventually caused coalescence of the voids. This proposed mechanism seems to suggest that the plasticizing effect is limited by the diffusion of water into the small voids in the matrix. The complex and rigid structure of CWMs may have hindered the plasticizing mechanism on its structural relaxation behavior and thus limiting the effect of moisture.

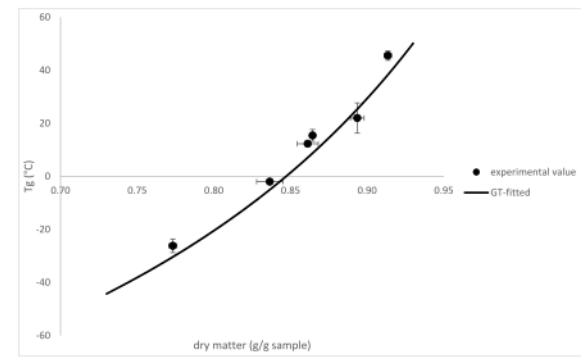


Fig. 2. Tg of lemon peel AIR as measured by DSC.

Table 3

Gordon-Taylor parameters from lemon peel CWM measured using different methods.

Materials	k	T _s (°C)
DSC		
AIR	4.81 \pm 0.83 ^a	117.2 \pm 17.5 ^a
TMCT		
AIR	0.67 \pm 0.10 ^b	43.16 \pm 2.55 ^b
Functionalized AR	0.59 \pm 0.15 ^b	37.36 \pm 3.24 ^c

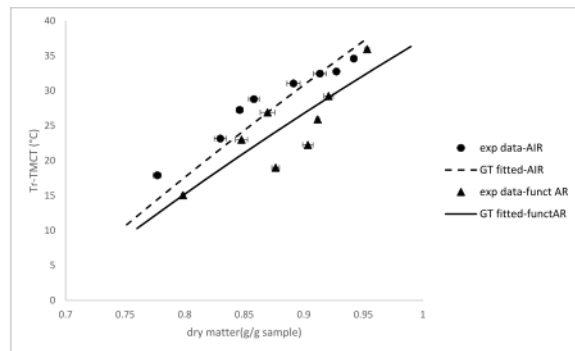


Fig. 3. Temperature of relaxation for AIR and functionalized AR from lemon peel as measured by TMCT.

When the Tr-TMCT values were fitted to the G-T equation, the values of anhydrous relaxation temperature (T_g) and k obtained were exceptionally low compared to the parameters obtained for the DSC based T_g curve (Table 3). This indicates that the material behavior reflected by the Tr-TMCT value change with moisture content is vastly different from the T_g values obtained by DSC. This may suggest that the two methods captured different mechanism of relaxation. This hypothesis will be substantiated further with the storage study results discussed in section 3.3. below. Based on the Tr-TMCT behavior and the fitted parameters value, the G-T equation may not be appropriate to describe the relaxation phenomena obtained by TMCT.

The result from the DMTA analysis, specifically the $\tan \delta$ curve in function of temperature, is presented (Fig. 4) to describe the structural relaxation phenomena of the lemon peel CWM residue. The storage (G')

and loss modulus (G'') curves in function of temperature are presented in the Supplementary Materials (Figure S-3). Comparable behavior of the moduli and loss factor as a function of temperature was observed for pea and soybean cotyledon (Ballesteros & Walters, 2011, 2019). They showed that over the range of -120 °C– 120 °C, the G' measured declined in the beginning (at low temperature) and started to increase from a certain temperature onwards. The G'' was constant in the beginning and started to increase towards a plateau, and $\tan \delta$ increased towards a plateau or a peak. The value of relaxation temperature (Tr-DMTA) generally could be determined by the peak of loss factor ($\tan \delta$) (Liu et al., 2006). However, the peak of the $\tan \delta$ in this study was difficult to be precisely determined, especially for samples with very low moisture content. Therefore, the structural relaxation phenomena will be discussed based on the behavior of the $\tan \delta$ curve. As a reference, the $\tan \delta$ curve of microcrystalline cellulose in function of temperature is presented in the Supplementary Materials (Figure S-4).

The $\tan \delta$ curve of lemon peel CWM, can be approximately divided into three regions: (i) a lower temperature range with the onset of $\tan \delta$ change (preceded by a constant value, especially for the low moisture systems) (ii) a medium temperature range with a steep increase of $\tan \delta$, and (iii) a final region where $\tan \delta$ reached its highest value and became constant or started to decline. At low temperature region (between -60 °C and 20 °C, with different range for samples with different moisture content), the $\tan \delta$ was mostly constant. As the CWM residue was heated, $\tan \delta$ started to increase (onset region) at a temperature between -30 °C and 20 °C. The increase of $\tan \delta$ upon heating suggests that the material started to lose its stiffness and a more plastic deformation could occur. The loss of stiffness continued at the second region with a steep increase of $\tan \delta$ and it reached a maximum point at temperature between 40 °C and 50 °C.

The plasticizing effect of moisture could be observed in the DMTA results based on the changes of $\tan \delta$ curve behavior. First, the absolute values of $\tan \delta$ increased with the increase in the moisture content of the samples. The increase of $\tan \delta$ after the onset region became more drastic as the moisture content in the sample increased and it occurred at lower temperatures for samples with higher moisture contents. Lastly, the maximum value of $\tan \delta$ was reached at lower temperatures as the moisture content of the samples increased. The $\tan \delta$ curve for AIR (Fig. 4A) and functionalized AR (Fig. 4B) showed very similar behavior. However, the plasticizing effect of moisture was more pronounced in the $\tan \delta$ curve of AIR, as also observed in the Tr-TMCT results.

In order to compare all methods of the transition/relaxation analysis, T_g and Tr-TMCT points were overlaid on the $\tan \delta$ curve (Fig. 4). DSC-based T_g values (based on AIR results) seem to be located approximately at the onset of the $\tan \delta$ change. On the other hand, Tr-TMCT values are located at around the middle (inflection point) of the rapidly increasing section of $\tan \delta$ curve (Fig. 4), coinciding with the lowest value of G' and on the point where G'' starts to increase (Figure S-3). Therefore, these points on the DMTA curves seems to indicate the onset of the change in compressibility of the material.

Tr-TMCT value of lemon peel CWM (AIR) at each moisture content was higher than the measurable T_g value from DSC, except for sample with the lowest moisture content (9% w.b.). This observation agrees with many studies that showed higher mechanical relaxation temperatures compared to the glass transition (Boonyai et al., 2006; Fan & Roos, 2017; Georget et al., 1998; Rahman et al., 2007). However, the temperature of transition for anhydrous material (T_g) obtained from the G-T equation fitted parameter was much lower for Tr-TMCT result (~ 40 °C) compared to DSC (117 °C). The huge difference in the anhydrous transition/relaxation temperature and the moisture plasticizing effect may indicate completely different transition/relaxation phenomena observed between the thermal and mechanical method of analysis. This raises the question of which temperature (structural relaxation or glass transition) is better suited to predict the storage stability of CWM.

The increasing $\tan \delta$ behavior suggests higher translational molecular mobility in the CWM residue which is suspected to have a

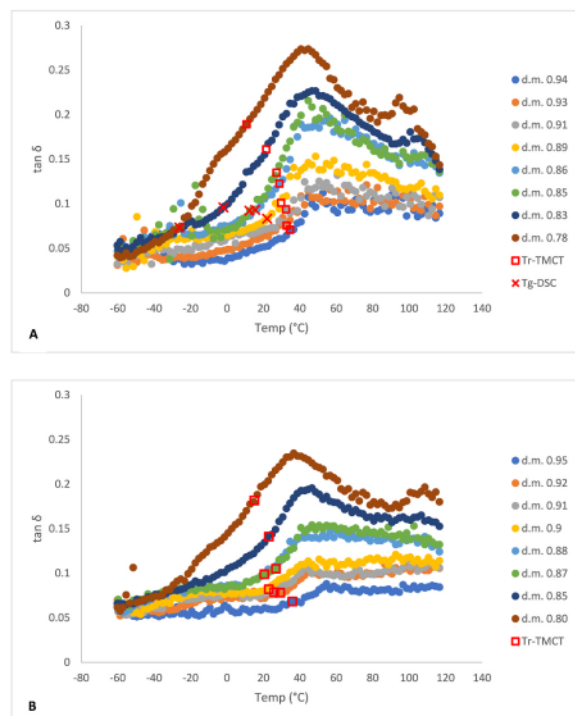


Fig. 4. Tan δ curve from DMTA analysis together with Tr-TMCT and T_g for (A) AIR and (B) Functionalized AR.

detrimental effect on the stability of the functionalized AR during storage. Higher molecular mobility increased the solid flow of molecules in the matrix of CWM which may induce collapse (Fan & Roos, 2017). Thus, a storage study was subsequently performed on the functionalized AR from lemon peel in order to corroborate whether the change in the behavior of $\tan \delta$ curve could be useful in predicting CWM residue's stability during storage. The behavior of the $\tan \delta$ curve depicted in Fig. 4 was used to determine different storage conditions that will cover different regions, from stable to unstable. Three temperature conditions were chosen, 10, 25 and 40 °C to represent the temperature before onset of $\tan \delta$ change, after onset when the $\tan \delta$ curve began to increase rapidly (but still below Tr-TMCT) and when the $\tan \delta$ curve almost reached its maximum value (above Tr-TMCT), respectively. Three moisture content values (11%, 14% and 16%) were selected, each corresponding to a different $\tan \delta$ curve profile to include the effect of water plasticization on the storage stability. An additional storage temperature of (-10) °C was added to the samples with highest moisture content to ensure that also in this case, a stable storage point (well before the onset of $\tan \delta$ change) was covered.

3.4. Storage stability and its relation to the molecular mobility

The storage stability study was focused on the change of the functionality of lemon peel CWM residue. Therefore, the rheological property, specifically G' , was measured to indicate the stability (or deterioration) of the texturizing potential of the functionalized AR. The values of G' throughout 14 weeks of storage are presented in Fig. 5. Samples stored at conditions before the onset of $\tan \delta$ change (at -10 °C and 10 °C) showed a stable G' up to 14 weeks of storage. When the storage temperature was higher than the onset of $\tan \delta$ change (at 25 °C and 40 °C), a significant decline in the G' -values was observed during storage. To quantify the rate of the G' decline or the rate of functionality loss during storage, the fractional conversion model was fitted to the results. The rate constant (k) values are presented in Table 4 below. The rate of the decline significantly increased as the storage temperature increased. Samples stored at 25 °C show a lower k -value compared to samples stored at 40 °C. However, after 14 weeks of storage, the G' value of samples stored at 25 °C declined significantly, reaching a similar value to the samples stored at 40 °C. On the other hand, samples stored at 40 °C already experienced a severe decline after 5 weeks of storage.

The samples stored at 25 °C showed a decline in G' value despite

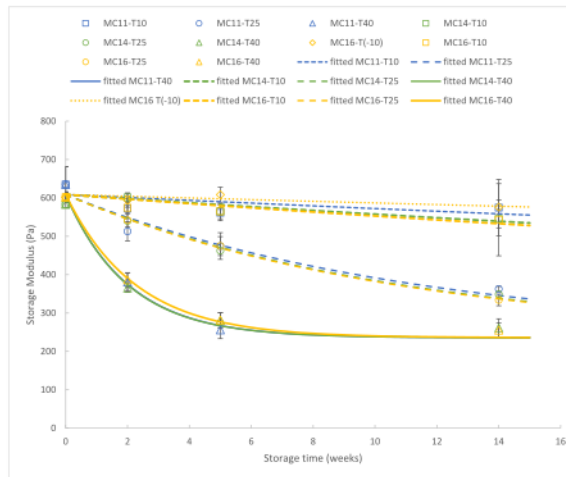


Fig. 5. Storage modulus (G') of CWM residue suspensions (2% d.m.) at ω 1 Hz from functionalized AR with different moisture content and storage temperature.

Table 4

Reaction rate constant (±approx. standard error) of the functionality loss during storage (14 weeks) for functionalized AR at different condition.

Storage condition	rate constant (k)	
Moisture content (%w.b)	Temperature (°C)	
11	10	0.010 ± 0.006^a
11	25	0.087 ± 0.013^b
11	40	0.493 ± 0.064^c
14	10	0.015 ± 0.004^a
14	25	0.091 ± 0.009^b
14	40	0.497 ± 0.073^c
16	-10	0.006 ± 0.002^a
16	10	0.016 ± 0.004^a
16	25	0.093 ± 0.003^b
16	40	0.441 ± 0.033^c

stored under the Tr-TMCT values, indicating that Tr-TMCT did not correspond to the stability of CWM functionality during storage. In conclusion, the relaxation phenomena described in the $\tan \delta$ curve correlate well to the storage stability of the lemon peel CWM. When the storage condition (temperature and moisture content) is located in the more progressed region of the $\tan \delta$ curve, which may indicate higher molecular mobility, the faster the decline on the G' . As long as the storage condition was kept below the onset of the $\tan \delta$ curve change, degradation of the functionality of the CWM residue was limited.

The declining G' during storage that happened when samples were stored at conditions where the $\tan \delta$ curve was increasing could be attributed to the structure collapse of the cell wall matrix. Such physical change could occur due to increasing molecular mobility when the material is transformed into a more viscous state (Fan & Roos, 2017). When $\tan \delta$ increased, stiffness of the molecules decreased which also suggests the reduction of the material viscosity to a level that is no longer sufficient to support the structure of the solid material. The increased viscous flow caused subsequent densification (Fan & Roos, 2017; To & Flink, 1978). In this case, the structural units (for example the repetitive element of the biopolymers in the CWM) can move independently from each other (Champion et al., 2000). Thus, interactions between cellulose microfibrils became possible which hindered the formation of an open CWM network that entraps water during the reconstitution of the material into suspension. Collapse of CWM, which could be prompted by many factors and treatments such as mechanical breaking (Van Audenhove et al., 2022) and chemical treatment, e.g. with alkaline solution, could lead to the reduction of CWM suspension's functionality. This transformation in the mechanical properties of solid materials may lead to substantial alterations of its performance in processing, storage stability, and sensory properties (Fan & Roos, 2017).

Previous study (Fernandez-Lopez et al., 2009) showed that degradation of the fiber-rich material functional properties, such as water binding capacity, became more severe as the moisture content increased during storage. Contrary, in this study, the rate of functionality loss (k -value) was not significantly different between samples stored at different moisture content (Table 4). At the same storage temperature, the moisture content of the samples (within the moisture content range studied) did not significantly affect the G' of the functionalized AR during storage. The plasticization effect of moisture was not pronounced in the storage study, contrary to common low-moisture food product behavior (Fan & Roos, 2017; Le Meste et al., 2002). As discussed previously, the limited moisture plasticizing effect, that was also observed in the results of TMCT-DMTA of CWM samples, was suspected to be caused by the composition of functionalized AR. Functionalized AR is composed mainly of cellulose and cellulose in its native form is a rigid polymer with some crystalline region in its structure, which may prevent the water migration into the particles and thus limit the moisture plasticizing effect. A NMR experiment which studied the effect of hydration on polymer mobility in onion CWM showed that water readily penetrated the pectin network and increased its mobility, whereas cellulose

mobility was unaffected by hydration (Hediger et al., 1999).

Furthermore, although the moisture plasticizing effect on the Tg of lemon peel CWM was clearly observed from the DSC results, this effect could not be seen in the storage study results. Larger differences between the storage temperature and Tg should normally cause faster deterioration of materials (Kymugasho et al., 2021; Roos, 1995; Zlatanović et al., 2019), however this phenomena also could not be observed in the results of the storage study. The substantial transition in the TMCT and DMTA result was not visible in the DSC thermogram for both AIR nor functionalized AR. However, this transition that is measurable by TMCT-DMTA and unmeasurable by the DSC seems to be the major driving force in the mechanical property changes of the material. Therefore, thermal glass transition obtained from DSC should not be considered an appropriate property to predict the stability of CWM residue, especially when being used as texturizing ingredient where the mechanical properties of the material is of ultimate importance.

4. Conclusion

The glass transition temperature of CWM has not been frequently reported due to the limitations of available methods of analysis. DSC has been widely used to predict the changes of materials during storage and its stability. However, DSC lacks sufficient sensitivity to measure the glass transition temperature of biopolymers such as CWMs. On the other hand, the change in mechanical properties measured by combined TMCT-DMTA analysis could reveal the structural relaxation phenomena of CWM based on the change of the compressibility and stiffness (loss factor/tan δ). Thus, the results from the TMCT-DMTA in this study could fill the gap as stability indicator that cannot be accomplished by DSC analysis of CWM. The relaxation phenomena observed by the mechanical property measurement, especially the tan δ curve from DMTA, is a more appropriate prediction to infer the stability of CWM, especially when used as texturizing ingredient where the rheological properties of the material is essential. In order to maintain stability of CWM residue, the storage condition (temperature and moisture) should be maintained below the onset region where tan δ curve started to increase. Conditions above the onset region of tan δ curve may indicate increased molecular mobility and lead to the degradation of the CWM rheological properties due to collapse. The ability of the TMCT-DMTA analysis to illustrate the relaxation phenomena could provide an opportunity for further study, for example on how processing could affect the behavior of the mechanical properties in order to design a shelf-stable functionalized CWM.

CRediT authorship contribution statement

Novita I. Putri: Writing – original draft, Visualization, Methodology, Investigation, Formal analysis, Data curation, Conceptualization. **Jelle Van Audenhove:** Writing – review & editing, Methodology. **Clare Kymugasho:** Methodology, Investigation. **Ann Loey:** Supervision, Resources, Methodology. **Marc Hendrickx:** Writing – review & editing, Supervision, Resources, Methodology, Funding acquisition, Conceptualization.

Declaration of competing interest

The authors declare that they have no known competing financial interests or personal relationships that could have appeared to influence the work reported in this paper.

Data availability

Data will be made available on request.

Acknowledgement

Novita Ika Putri is a PhD fellow funded through collaboration with

Cargill R&D Centre Europe. Jelle Van Audenhove is a postdoctoral researcher funded by the Internal Research Fund KU Leuven [grant number PD/MT2/22/052]. The funding source had no role in the study design, collection, analysis and interpretation of the data, the writing of this manuscript or in the decision to submit the manuscript for publication.

Appendix A. Supplementary data

Supplementary data to this article can be found online at <https://doi.org/10.1016/j.foodhyd.2023.109711>.

References

Andrade, P. R. D., Lemus, M. R., & Pérez, C. C. E. (2011). Models of sorption isotherms for food: Uses and limitations. *Vitae*, 18(3), 325–334. <https://doi.org/10.17533/udea.vitae.10682>

Aravindakshan, S., Kymugasho, C., Tafire, H., Van Loey, A., Grauwet, T., & Hendrickx, M. E. (2022). The moisture plasticizing effect on enzyme-catalyzed reactions in model and real systems in view of legume ageing and their hard to cook development. *Journal of Food Engineering*, 314(July 2021), Article 110781. <https://doi.org/10.1016/j.jfoodeng.2021.110781>

Ballesteros, D., & Walters, C. (2011). Detailed characterization of mechanical properties and molecular mobility within dry seed glasses: Relevance to the physiology of dry biological systems. *The Plant Journal*, 68(4), 607–619. <https://doi.org/10.1111/j.1365-313X.2011.04711.x>

Ballesteros, D., & Walters, C. (2019). Solid-state biology and seed longevity: A mechanical analysis of glasses in pea and soybean embryonic axes. *Frontiers in Plant Science*, 10(July), 1–12. <https://doi.org/10.3389/fpls.2019.00920>

Boonyai, P., Bhandari, B., & Howes, T. (2006). Applications of thermal mechanical compression tests in food powder analysis. *International Journal of Food Properties*, 9(1), 127–134. <https://doi.org/10.1080/10942910500473988>

Champion, D., Le Meste, M., & Simatos, D. (2000). Towards an improved understanding of glass transition and relaxations in foods: Molecular mobility in the glass transition range. *Trends in Food Science and Technology*, 11(2), 41–55. [https://doi.org/10.1016/S0924-2244\(00\)00479](https://doi.org/10.1016/S0924-2244(00)00479)

Fan, F., & Roos, Y. H. (2017). Glass transition-associated structural relaxations and applications of relaxation times in amorphous food solids: A review. *Food Engineering Reviews*, 9(4), 257–270. <https://doi.org/10.1016/S12393-017-9166-6>

Fernandez-Lopez, J., Sendra-Nadal, E., Navarro, C., Sayas, E., Viuda-Martos, M., & Pérez-Alvarez, J. A. (2009). Storage stability of a high dietary fibre powder from orange by-products. *International Journal of Food Science and Technology*, 44, 748–756.

Fongin, S., Kawai, K., Hamakusumairi, N., & Hagura, Y. (2017). Effects of water and maltodextrin on the glass transition temperature of freeze-dried mango pulp and an empirical model to predict plasticizing effect of water on dried fruits. *Journal of Food Engineering*, 210, 91–97. <https://doi.org/10.1016/j.jfoodeng.2017.04.025>

Georget, D. M. R., Smith, A. C., & Waldron, K. W. (1998). Low moisture thermo-mechanical properties of carrot cell wall components. *Thermochimica Acta*, 315(1), 51–60. [https://doi.org/10.1016/S0040-6031\(98\)00276-7](https://doi.org/10.1016/S0040-6031(98)00276-7)

Georget, D. M. R., Smith, A. C., & Waldron, K. W. (1999). Thermal transitions in freeze-dried carrot and its cell wall components. *Thermochimica Acta*, 332(2), 203–210. [https://doi.org/10.1016/S0040-6031\(99\)00075-1](https://doi.org/10.1016/S0040-6031(99)00075-1)

Greenspan, L. (1976). Humidity fixed points of binary saturated aqueous solutions. *Journal of Research of the National Bureau of Standards - A Physics and Chemistry*, 81A(1), 89–96.

Hediger, S., Emley, L., & Fischer, M. (1999). Solid-state NMR characterization of hydration effects on polymer mobility in onion cell-wall material. *Carbohydrate Research*, 322(1–2), 102–112. [https://doi.org/10.1016/S0008-6215\(99\)00195-0](https://doi.org/10.1016/S0008-6215(99)00195-0)

Kilburn, D., Claude, J., Mezzenga, R., Dubé, G., Alami, A., & Ubbink, J. (2004). Water in glassy carbohydrates: Opening it up at the nanolevel. *Journal of Physical Chemistry B*, 108(33), 12436–12441. <https://doi.org/10.1021/jp048774f>

Koç, B., Yilmazer, S. S., Balkır, P., & Ertekin, F. K. (2010). Moisture sorption isotherms and storage stability of spray-dried yogurt powder. *Drying Technology*, 28(6), 816–822. <https://doi.org/10.1080/07373937.2010.485083>

Kymugasho, C., Kamau, P. G., Aravindakshan, S., & Hendrickx, M. E. (2021). Evaluation of storage stability of low moisture whole common beans and their fractions through the use of state diagrams. *Food Research International*, 140(July 2020), Article 109794. <https://doi.org/10.1016/j.foodres.2020.109794>

Le Meste, M., Champion, D., Roudaut, G., Blond, G., & Simatos, D. (2002). Glass transition and food technology: A critical appraisal. *Journal of Food Science*, 67(7), 2444–2458. <https://doi.org/10.1111/j.1365-2621.2002.tb08758.x>

Lee, D. S., & Robertson, G. L. (2022). Shelf-life estimation of packaged dried foods as affected by choice of moisture sorption isotherm models. *Journal of Food Processing and Preservation*, 46, Article e16335. <https://doi.org/10.1111/jfpp.16335>

Liu, Y., Bhandari, B., & Zhou, W. (2006). Glass transition and enthalpy relaxation of amorphous food saccharides: A review. *Journal of Agricultural and Food Chemistry*, 54(16), 5701–5717. <https://doi.org/10.1021/jf060188r>

Nieto-Calvache, J., Pla, M. de E., & Gershenson, L. N. (2019). Dietary fibre concentrates produced from papaya by-products for agroindustrial waste valorisation. *International Journal of Food Science and Technology*, 54, 1074–1080.

Pelgrom, P. J. M., Schutyser, M. A. I., & Boom, R. M. (2013). Thermomechanical morphology of peas and its relation to fracture behaviour. *Food and Bioprocess Technology*, 6(12), 3317–3325. <https://doi.org/10.1007/s11947-012-1031-2>

Putri, N. I., Celus, M., Van Audenhove, J., Nanseera, R. P., Van Loey, A., & Hendrickx, M. (2022). Functionalization of pectin-depleted residue from different citrus by-products by high pressure homogenization. *Food Hydrocolloids*, 129(March), Article 107638. <https://doi.org/10.1016/j.foodhyd.2022.107638>

Quirijns, E. J., Van Boxtel, A. J. B., Van Looy, W. K. P., & Van Straten, G. (2005). Sorption isotherms, GAB parameters and isosteric heat of sorption. *Journal of the Science of Food and Agriculture*, 85(11), 1805–1814. <https://doi.org/10.1002/jsfa.2140>

Rahman, M. S., Al-Marhubi, I. M., & Al-Mahrouqi, A. (2007). Measurement of glass transition temperature by mechanical (DMTA), thermal (DSC and mdsc), water diffusion and density methods: A comparison study. *Chemical Physics Letters*, 440 (4–6), 372–377. <https://doi.org/10.1016/j.cplett.2007.04.067>

Roos, Y. (1995). Characterization of food polymers using state diagrams. *Journal of Food Engineering*, 24, 339–360.

Roos, Y. H. (1998). Phase transitions and structure of solid food matrices. *Current Opinion in Colloid & Interface Science*, 3(6), 651–656. [https://doi.org/10.1016/S1359-0294\(98\)80095-2](https://doi.org/10.1016/S1359-0294(98)80095-2)

Sablani, S. S., Kasapis, S., & Rahman, M. S. (2007). Evaluating water activity and glass transition concepts for food stability. *Journal of Food Engineering*, 78(1), 266–271. <https://doi.org/10.1016/j.jfoodeng.2005.09.025>

Sablani, S. S., Syamaladevi, R. M., & Swanson, B. G. (2010). A review of methods, data and applications of state diagrams of food systems. *Food Engineering Reviews*, 2(3), 168–203. <https://doi.org/10.1007/s1293-010-9020-6>

Sant'Anna, V., Englert, A. H., Corrêa, A. P. F., Brandelli, A., Ferreira Marczak, L. D., & Tessaro, I. C. (2014). Grape marc powder: Physicochemical and microbiological stability during storage and moisture sorption isotherm. *Food and Bioprocess Technology*, 7(9), 2500–2506. <https://doi.org/10.1007/s11947-013-1198-1>

Sharma, P. C., Gupta, A., & Issar, K. (2017). Effect of packaging and storage on dried apple pomace and fiber extracted from pomace. *Journal of Food Processing and Preservation*, 41(3), 1–10. <https://doi.org/10.1111/jfpp.12913>

Sormoli, M. E., & Langrish, T. A. G. (2015). Moisture sorption isotherms and net isosteric heat of sorption for spray-dried pure orange juice powder. *Lwt*, 62(1), 875–882. <https://doi.org/10.1016/j.lwt.2014.09.064>

Stepien, A., Witczak, M., & Witczak, T. (2020). Sorption properties, glass transition and state diagrams for pumpkin powders containing maltodextrins. *Lwt*, 134(May). <https://doi.org/10.1016/j.lwt.2020.110192>

Timmermann, E. O., Chirife, J., & Iglesias, H. A. (2001). Water sorption isotherms of foods and foodstuffs: BET or GAB parameters? *Journal of Food Engineering*, 48(1), 19–31. [https://doi.org/10.1016/S0260-8774\(00\)0139-4](https://doi.org/10.1016/S0260-8774(00)0139-4)

To, E. C., & Flink, J. M. (1978). 'Collapse', a structural transition in freeze dried carbohydrates: II. Effect of solute composition. *J. Fd Technol.*, 13(6), 583–594. <https://doi.org/10.1111/j.1365-2621.1978.tb00837.x>

Van Audenhove, J., Bernaerts, T., Putri, N., Van Rooy, L., Van Loey, A., & Hendrickx, M. (2022). The role of mechanical collapse by cryogenic ball milling on the effect of high-pressure homogenization on the microstructural and texturizing properties of partially pectin-depleted tomato cell wall material. *Food Research International*, 155 (December 2021), Article 111033. <https://doi.org/10.1016/j.foodres.2022.111033>

Willemsen, K. L. D. D., Panizzo, A., Moelants, K., Cardinaels, R., Wallecan, J., Moldenaers, P., & Hendrickx, M. (2018). Effect of pH and salts on microstructure and viscoelastic properties of lemon peel acid insoluble fiber suspensions upon high pressure homogenization. *Food Hydrocolloids*, 82, 144–154. <https://doi.org/10.1016/j.foodhyd.2018.04.005>

Willemsen, K. L. D. D., Panizzo, A., Moelants, K., Debon, S. J. J., Desmet, C., Cardinaels, R., Moldenaers, P., Wallecan, J., & Hendrickx, M. E. G. (2017). Physico-chemical and viscoelastic properties of high pressure homogenized lemon peel fiber fraction suspensions obtained after sequential pectin extraction. *Food Hydrocolloids*, 72, 358–371. <https://doi.org/10.1016/j.foodhyd.2017.06.020>

Zlatanović, S., Ostožić, S., Micić, D., Rankov, S., Dodevska, M., Vukosavljević, P., & Gorjanović, S. (2019). Thermal behaviour and degradation kinetics of apple pomace flours. *Thermochimica Acta*, 673(January), 17–25. <https://doi.org/10.1016/j.tca.2019.01.009>

paper 2

ORIGINALITY REPORT



PRIMARY SOURCES

- 1 **J. Van Audenhove, N.I. Putri, I. Caveye, A.M. Van Loey, M.E. Hendrickx. "The impact of drying and storage in the semi-dry state on the texturizing potential of partially pectin-depleted tomato cell wall material functionalised by high-pressure homogenisation", Food Hydrocolloids, 2023**
Publication
- 2 **tr.scribd.com**
Internet Source
- 3 **web5.arch.cuhk.edu.hk**
Internet Source
- 4 **"Water Properties in Food, Health, Pharmaceutical and Biological Systems: ISOPOW 10", Wiley, 2010**
Publication
- 5 **daneshyari.com**
Internet Source
- 6 **mro.massey.ac.nz**
Internet Source

7

research.tue.nl

Internet Source

1 %

8

Shruti Aravindakshan, Thi Hoai An Nguyen, Clare Kyomugasho, Ann Van Loey, Marc E. Hendrickx. "The rehydration attributes and quality characteristics of 'Quick-cooking' dehydrated beans: Implications of glass transition on storage stability", Food Research International, 2022

1 %

Publication

9

link.springer.com

Internet Source

1 %

Exclude quotes

Off

Exclude matches

< 1%

Exclude bibliography

On